Adenovirus-mediated knockdown of activin A receptor type 2A attenuates immune-induced hepatic fibrosis in mice and inhibits interleukin-17-induced activation of primary hepatic stellate cells

HONGJUN ZHANG[1], BAOLING JU[1], YING NIE[1], BAOHUI SONG[1], YUANHONG XU[1] and PING GAO[2]

[1]Department of Immunology, Mudanjiang Medical University, Mudanjiang, Heilongjiang 157011;
[2]Department of Gastroenterology, Mudanjiang Forestry Central Hospital, Mudanjiang, Heilongjiang 157000, P.R. China

Abstract. Fibrosis induces a progressive loss of liver function, thus leading to organ failure. Activins are secreted proteins that belong to the transforming growth factor (TGF)-β superfamily, which initiate signaling by binding to their two type II receptors: Activin A receptor type 2A (ACVR2A) and activin A receptor type 2B. Previous studies that have explored the mechanisms underlying immune-induced hepatic fibrosis have mainly focused on TGF-β signaling, not activin signaling. To investigate the role of the activin pathway in this disease, adenovirus particles containing short hairpin (sh)RNA targeting ACVR2A mRNA (Ad-ACVR2A shRNA) were administered to mice, which were chronically treated with concanavalin A (Con A). The pathological changes in the liver were evaluated with hematoxylin/eosin staining, Masson trichrome staining and immunohistochemical assay. The results detected an increase in serum activin A and liver ACVR2A in Con A-treated animals. Conversely, liver function was partially restored and fibrotic injury was attenuated when activin signaling was blocked. In addition, the activation of hepatic stellate cells (HSCs) in response to Con A was suppressed by Ad-ACVR2A shRNA, as evidenced by decreased α-smooth muscle actin, and type I and IV collagen expression. Furthermore, primary mouse HSCs (mHSCs) were activated when exposed to interleukin (IL)-17A or IL-17F, which are two major cytokines produced by cluster of differentiation 4+ T helper 17 cells. The levels of activin A, type I and IV collagen were determined with ELISA kits and the expression of fibrotic molecules was determined with western blot analysis. Conversely, blocking activin/ACVR2A impaired the potency of HSCs to produce collagens in response to IL-17s. In addition, C terminus phosphorylation of Smad2 on Ser465 and Ser467, induced by either Con A in the liver or by IL-17s in mHSCs, was partly inhibited when activin A/ACVR2A signaling was suppressed. Collectively, the present study demonstrated an involvement of activated activin A/ACVR2A/Smad2 signaling in immune-induced hepatic fibrosis.

Introduction

Hepatic fibrosis is defined as the aberrant and excess production of extracellular matrix (ECM) components, which is involved in numerous human chronic liver diseases (CLDs) (1). Although fibrogenesis is considered a potentially reversible scarring response in the liver, persistent fibrosis can lead to progressive loss of organ function and subsequent liver failure (2). Furthermore, immune dysregulation occurs in several liver diseases, including autoimmune hepatitis, alcohol-related liver disease and primary biliary cirrhosis (1). Progress in determining the underlying mechanisms of immune-induced liver fibrogenesis has given realistic hopes to patients with CLD; however, scientific and clinical challenges remain (3).

Hepatic stellate cells (HSCs) have garnered attention because they give rise to ~90% of ECM-generating myofibroblasts during hepatic fibrosis (4). In addition to repetitive injury of hepatocytes and inflammation following destructive stimulation, the activation/proliferation of HSCs is a major mechanism that contributes to hepatic fibrosis (5). There is a growing consensus that HSCs may function as recipients of inflammatory signals, and thus generate fibrogenic cytokines, including transforming growth factor (TGF)-β (6). Persistently activated TGF-β signaling leads to overproduction of ECM by HSCs in the liver (7). Conversely, inhibition of TGF-β signaling can attenuate dimethylnitrosamine-induced liver fibrosis, but fails to completely abrogate it (8,9), thus indicating that TGF-β may not be the sole regulator in fibrotic diseases.

Activins are another important TGF-β-like group in the TGF-β superfamily (10). Similar to TGF-βs, activins, including activin A, B, AB and AC, are secreted proteins formed by various activin subunits as homo- and heterodimers (11). Activins signal by binding to heteromeric complexes, which

consist of type I and II receptors (11). Activin A receptor type 2A (ACVR2A, formerly known as ACTRII) is an essential type II receptor for activin (10). Notably, increased expression of activin A in cirrhotic and fibrotic liver tissues has previously been reported (12). Inhibition of activin A with its main biological inhibitor follistatin mitigates carbon tetrachloride (CCl$_4$)-induced hepatic fibrosis (13). These studies suggest a contributory role for activated activin signaling in hepatic fibrosis. However, the precise mechanisms underlying activin-mediated events in hepatic fibrosis, particularly with regards to immune-mediated fibrosis, remain to be fully elucidated.

In response to injurious stimuli, HSCs interact closely with liver-resident cells such as hepatocytes, endothelial cells and Kupffer cells, and with infiltrating immune cells, such as cluster of differentiation (CD)4$^+$ T lymphocytes (14). Concanavalin A (Con A) is a plant lectin, multiple injections of which induce T-cell-mediated liver fibrosis in mice (15). In addition, it has been suggested that Con A administration promotes the infiltration and differentiation of T helper (Th)17 cells in the liver (16). Interleukin (IL)-17 is mainly generated by Th17 cells and has been reported to accelerate liver fibrosis by activating HSCs (17). However, whether activin signaling has a role in Th17-mediated HSC activation is unclear and requires further investigation.

In the present study, T-cell-mediated liver fibrosis was established in BALB/c mice following numerous injections of Con A. To disrupt activin signaling delivery, recombinant adenoviruses expressing ACVR2A short hairpin (sh)RNA were administered to experimental animals and primary mouse HSCs (mHSCs). In addition, IL-17A and IL-17F, two important Th17-family cytokines, were used to stimulate mHSCs expressing normal or decreased ACVR2A. The results indicated that inhibition of the activin signaling pathway attenuated Con A-induced fibrotic injury in the liver and suppressed IL-17-induced mHSC activation.

Materials and methods

Animal model. BALB/c mice (weight, 20-23 g; age, 8-10 weeks) were purchased from Liaoning Changsheng Biotech Co., Ltd. (Benxi, China) and maintained under a 12-h light/dark cycle with free access to food and water. The present study was approved by the Institutional Animal Care and Use committee of Mudanjiang Medical University (Mudanjiang, China).

The whole experiment consisted of two parts. In experiment part 1, a total of 16 mice were randomly divided into two groups: i) Control (n=8) and ii) Con A (n=8) groups. For establishment of the immune-associated hepatic fibrosis animal model, mice in the Con A group were administered intravenous (i.v.) injections of Con A (8 mg/kg/week; Sigma-Aldrich; Merck KGaA, Darmstadt, Germany) through the tail vein for up to 6 weeks (18). The mice were anesthetized by pentobarbital sodium (50 mg/kg body weight; intraperitoneal injection; Xiya Reagent, Linshu, China), and the blood was obtained from the retro-orbital plexus. The blood was then centrifuged at 850 x g for 10 min (4°C) to collect the serum. After sacrifice, the liver was removed from each animal. The expression levels of activin A, ACVR2A, IL-17A and IL-17F were subsequently detected.

In experiment part 2, a total of 40 mice were randomly divided into five groups (n=8 per group): i) Control, ii) Con A, iii) ConA + Ad-negative control (NC) shRNA, iv) ConA + Ad-ACVR2A shRNA, v) control + Ad-NC shRNA. Recombinant adenoviruses carrying ACVR2A shRNA (Ad-ACVR2A shRNA, target area: 5'-GGAGUGUCUUUUCUUUAAU-3'; NM_007396.4) (19) and NC shRNA (Ad-NC shRNA) (Shanghai GenePharma Co., Ltd., Shanghai, China) were used in the present study. Hepatic fibrosis was induced in mice in groups 2-4 as aforementioned. At weeks 1 and 4, 1x10^9 plaque-forming units Ad-ACVR2A shRNA or Ad-NC shRNA was administered to mice in groups 3-5 via i.v. injection 24 h after Con A injection. Serum and liver tissue samples were obtained from each mouse at the end of week 6, and stored at -80°C or embedded into paraffin until use.

Cell culture. Primary mHSCs were isolated from the fresh liver samples of BALB/c mice according to previously reported protocols (20-23) with minor modifications. Briefly, the liver samples were initially perfused with PBS containing heparin (2 U/ml) at 4°C for ~20 min, and were then digested with a mix of pronase (1 mg/ml; Dalian Meilun Biotech Co., Ltd., Dalian, China)/collagenase IV (0.4 mg/ml; Invitrogen; Thermo Fisher Scientific, Inc., Waltham, MA, USA)/DNase I (0.2 mg/ml; Invitrogen; Thermo Fisher Scientific, Inc.) at 37°C for ~30 min. Subsequently, tissue samples were cut into small pieces and incubated with warm PBS containing pronase (1 mg/ml)/collagenase IV (0.4 mg/ml)/DNase I (0.2 mg/ml) at 37°C for additional 15 min. The digestion was terminated by the addition of an equal volume of Dulbecco's modified Eagle's medium (DMEM; Gibco; Thermo Fisher Scientific, Inc.) containing 10% fetal bovine serum (FBS; HyClone; GE Healthcare, Logan, UT, USA). The digested mix was filtered and centrifuged at 160 x g at 4°C for 3 min, and the supernatant was discarded. The cell pellet was resuspended in PBS, and centrifuged again. Subsequently, cells suspended in DMEM were carefully added to 5 ml 39.5% percoll solution (Beijing Solarbio Science & Technology Co., Ltd., Beijing, China) and were centrifuged at 430 x g at 4°C for 20 min. The interface between DMEM and percoll solution was collected, suspended in DMEM, and centrifuged at 160 x g at 4°C for 7 min to collect the final cell pellet. The cells were then cultured with DMEM containing penicillin/streptomycin and 10% FBS. The purity of HSCs was >90%, as determined by desmin immunostaining (24). The first passage of mHSCs was used in the present study. Recombinant murine IL-17A and IL-17F (PeproTech, Inc., Rocky Hill, NJ, USA) at 10, 30 or 100 ng/ml were used to stimulate mHSCs for 1, 3, 6, 12, 24 or 48 h. For some experiments, the mHSCs were infected with Ad-ACVR2A shRNA or Ad-NC shRNA (multiplicity of infection, both 50) for 24 h, and were then stimulated with recombinant IL-17A (30 ng/ml) or IL-17F (30 ng/ml) for additional 48 h.

Western blot analysis. Total proteins were isolated from liver tissues and primary HSCs using radioimmunoprecipitation assay lysis buffer (P0013B), and protein concentration was quantified using a Bicinchoninic Acid Protein assay kit (P0009) (both from Beyotime Institute of Biotechnology,

Table I. Sequences of primers used in reverse transcription-quantitative polymerase chain reaction analysis.

Gene name	Sequence (5'>3')	Product (bp)	Gene ID
ACVR2A	F: AAGATAAACGGCGACATTG R: GTAACAGGATTTGAAGTGGG	232	NM_007396.4
ACTA2	F: CCGCAAATGCTTCTAAGTCCC R: AATTGAATCAGTGTTGCTAGGC	195	NM_007392.3
COL1A1	F: GGCAAGACAGTCATCGAATACA R: GAGGGAGTTTACACGAAGCAG	137	NM_007742.4
COL4A1	F: CGGCTATTCCTTCGTGATG R: ATGGCGTGGGCTTCTTGA	206	NM_009931.2
β-actin	F: CTGTGCCCATCTACGAGGGCTAT R: TTTGATGTCACGCACGATTCC	155	NM_007393.5

ACTA2, actin α2; ACVR2A, activin A receptor type 2A; COL1A1, collagen type I α1 chain; COL4A1, collagen type IV α1 chain F, forward; R, reverse.

Shanghai, China). Rabbit polyclonal antibodies against ACVR2A (ab135634, 1:500; Abcam, Cambridge, UK), type I α collagen (collagen I, BA0325, 1:400; Wuhan Boster Biological Technology, Ltd., Wuhan, China), type IV α collagen (collagen IV, BA2174, 1:400; Wuhan Boster Biological Technology, Ltd.), Smad2 (bs-0718R, 1:500), phosphorylated (p)-Smad2$^{S465/467}$ (bs-3419R, 1:500; both from BIOSS, Beijing, China) and a mouse monoclonal antibody against α-smooth muscle actin (α-SMA, BM0002, 1:400; Wuhan Boster Biological Technology, Ltd.) were used to detect the expression of corresponding proteins. Briefly, equal protein samples (20 μg) mixed with loading buffer were separated by 10% SDS-PAGE for 2.5 h and were then transferred onto polyvinylidene fluoride membranes, which were blocked with 5% (M/V) non-fat milk (TTBS buffered) for 1 h at room temperature. The membranes were then incubated with primary antibodies at 4°C overnight, followed by incubation with goat anti-rabbit or goat anti-mouse horse-radish peroxidase (HRP)-labeled-immunoglobulin G (IgG) secondary antibodies (A0216 or A02087; 1: 5,000; Beyotime Institute of Biotechnology) for 45 min at 37°C. Finally, the membranes were visualized using an enhanced chemiluminescence reagent (Beyotime Institute of Biotechnology) in the dark. β-actin served as the control (sc-47778; 1:1,000; Santa Cruz Biotechnology, Inc., Dallas, Texas, USA). The software used to semi-quantify the blots was gel-pro analyzer (version 4).

Morphological structure analysis and immunohistochemistry (IHC). Staining reagents were purchased from Sinopharm Chemical Reagent Co., Ltd. (Beijing, China) or Beijing Solarbio Science & Technology Co., Ltd. Briefly, the liver tissues were first fixed in 4% paraformaldehyde (Sinopharm Chemical Reagent Co., Ltd.) at room temperature for 24 h, and then rinsed with water for 4 h. After being dehydrated in an alcohol gradient (70, 80, 90 and 100%), the tissues were embedded into paraffin. The tissue block was cut into 5-μm slices, slowly spread in water, and dried at 60°C for ~40 min. Subsequently, the tissue sections were dewaxed in xylene,

rehydrated in an alcohol gradient (95, 85 and 75% for 2 min, respectively) and soaked in water for 2 min. The sections were then treated with staining reagents accordingly to the manufacturer's protocols. For hematoxylin and eosin (H&E) staining, the prepared tissue sections were stained with hematoxylin for 5 min and with eosin for 3 min. The collagen areas were stained blue using Masson trichrome. In brief, the slices were stained with acid ponceau/solferino for 1 min and then with aniline blue for 5 min at room temperature. Cell nuclei were stained with hematoxylin for 6 min. The main by-product of collagens, hydroxyproline, was detected in fresh liver tissues using a commercial detection kit (A030-1; Nanjing Jiancheng Bioengineering Institute, Nanjing, China) according to the manufacturer's protocol.

For IHC, tissue sections were incubated in citrate buffer at 100°C for 10 min for antigen retrieval, and then with 3% H_2O_2 at room temperature for 15 min to block peroxidase activity. After washing, sections were treated with goat serum (SL2-10; Beijing Solarbio Science & Technology Co., Ltd.) for 15 min, and then with rabbit polyclonal antibodies against α-SMA (BS-0189R, 1:200; BIOSS), collagen I (BA0325, 1:200) and collagen IV (BA2174, 1:200) (both from Wuhan Boster Biological Technology, Ltd.) at 4°C overnight under humid conditions. These samples were then treated with biotin-labeled goat anti-rabbit IgG (A0277; 1:200; Beyotime Institute of Biotechnology) at 37°C for 30 min, and then with HRP-labeled streptavidin (both from Beyotime Institute of Biotechnology) for another 30 min. After visualization with DAB (Beijing Solarbio Science & Technology Co., Ltd.), images of the tissue sections were captured under a microscope (BX53; Olympus, Tokyo, Japan).

Reverse transcription-quantitative real-time polymerase chain reaction (RT-qPCR). Primers used for detection of the mRNA expression levels of ACVR2A, actin α2 (ACTA2), collagen type I α1 chain (COL1A1) and collagen type IV α1 chain (COL4A1) genes are listed in Table I. Total RNA was isolated from liver samples and cells using the RNApure extraction kit (RP1201), after which RNA was reverse tran-

scribed into cDNA using Super M-MLV reverse transcriptase (PR6502) (both from BioTeke Corporation, Beijing, China) according to the manufacturer's protocol. Subsequently, qPCR was performed in a mix containing primer pairs (10 μM, 0.5 μl of each), cDNA (1 μl), SYBR-Green mastermix (10 μl, SY1020; Beijing Solarbio Science & Technology Co., Ltd.) and ddH$_2$O (8 μl) on an Exicycler™ 96 real-time quantitative thermal block (Bioneer Corporation, Daejeon, South Korea). The relative mRNA expression levels of each gene were calculated using the $2^{-\Delta\Delta Cq}$ method (25). β-actin was used as a control. The thermocycling conditions were as follows: 94°C for 5 min, 38 cycles at 94°C for 15 sec / 60°C for 20 sec / 72°C for 30 sec, 72°C for 150 sec, 40°C for 90 sec, melting from 60°C to 94°C (every 1°C for 1 sec), 25°C for 60-120 sec.

Assessment of serum or cell supernatant indices. The contents of activin A, IL-17A and IL-17F in the serum, and the contents of collagen I and IV in cell supernatants were determined using corresponding ELISA kits (EK0302/EK0431/EK0796; Boster and SEA571Mu/SEA180Mu; Uscn Life Sciences, Inc., Wuhan, China) according to the manufacturers' protocols. The activities of aspartate aminotransferase (AST) and alanine aminotransferase (ALT) were assessed using commercial detection kits (C010-1/C009-1; Nanjing Jiancheng Bioengineering Institute) according to the manufacturer's protocols.

Statistical analysis. The experiments were repeated for 3 times. Data are expressed as the means ± standard deviation or standard error. SPSS 20.0 software (IBM Corp., Armonk, NY, USA) was used to analyze the results. Data with equal variance between two groups were analyzed using Mann-Whitney test, whereas those with unequal variance were analyzed using a Student's t-test. Data over three groups were analyzed via one-way analysis of variance (ANOVA) and Bonferroni post hoc test. P<0.05 was considered to indicate a statistically significant difference.

Results

Con A administration stimulates activation of activin and IL-17 signaling in the liver. In the present study, liver and serum samples were collected from the control and chronic Con A-treated mice at the end of week 6 (Fig. 1A). The contents of activin A, and IL-17A and IL-17F in the serum and liver tissue samples were detected using corresponding ELISA kits. Activin A levels were increased in Con A-treated mice compared with in the control mice (Fig. 1B). Increases in serum IL-17A and IL-17F levels were also detected in Con A-treated mice (Fig. 1C). Similar increases in expression were detected for these three indices in liver tissues (Fig. 1D and E).

The mRNA and protein expression levels of ACVR2A were also upregulated in liver tissues obtained from Con A-treated mice, as determined by RT-qPCR and western blot analysis (Fig. 1F and G). Subsequently, adenovirus particles containing ACVR2A shRNA or NC shRNA were intravenously injected into mice in the Con A group (Fig. 1H). The results demonstrated that Ad-NC shRNA did not affect the expression of ACVR2A in mice with or without liver fibrosis, whereas Ad-ACVR2A shRNA significantly inhibited ACVR2A expression in fibrotic liver tissue (Fig. 1I).

Adenovirus-mediated inhibition of ACVR2A attenuates Con A-induced liver fibrosis. To detect whether inhibition of ACVR2A may preserve liver function of Con A-treated mice, the activities of ALT and AST, which are transaminases critical for liver function, were tested in serum samples using the corresponding kits. The results indicated that ALT and AST activities were increased in mice treated with Con A compared with in the control group (Fig. 2A). Conversely, treatment with Ad-ACVR2A shRNA, but not Ad-NC shRNA, partly rescued the impaired liver function, as evidenced by decreased ALT and AST activities (Fig. 2A). The results of H&E staining demonstrated that mice in the control group exhibited normal and clear lobular architecture, and the hepatic cells were arranged in neat rows (Fig. 2B). However, apparent pathological alterations were detected in the livers of Con A-treated mice. The hepatic cord was disarranged and inflammatory cells abnormally infiltrated into the liver (Fig. 2B). The pathological situation was not improved by treatment with Ad-NC shRNA; however, it was partly improved by Ad-ACVR2A shRNA treatment, although not completely (Fig. 2B). Furthermore, liver fibrosis was detected using Masson trichrome staining; evident collagen deposition was observed in liver samples from Con A-treated mice (Fig. 2C). Adenovirus-mediated blockade of activin signaling had an antifibrotic effect in the liver (Fig. 2C). In addition, downregulation of hydroxyproline in Ad-ACVR2A shRNA-treated mice also confirmed the reduced liver fibrosis (Fig. 2D). Notably, in one of the control groups, mice received two injections of Ad-NC shRNA, in order to investigate whether the adenoviruses used in the present study had any adverse effects on the mice. There were no significant alterations in liver structure and function between normal control mice and those treated with Ad-NC shRNA. Collectively, these results indicated that abnormal activation of the activin/ACVR2A signaling pathway may contribute to immune-associated fibrosis.

Inhibition of activin/ACVR2A signaling suppresses Con A-induced activation of HSCs in vivo. Excessive collagen deposition indicates abnormal fibrosis in the liver. The majority of ECM-generating myofibroblasts in the liver are derived from activated HSCs, and α-SMA is a molecular marker for activated HSCs (26). In the present study, the mRNA expression levels of ACTA2, COL1A1 and COL4A1 were determined using RT-qPCR, and the expression levels of their respective proteins, α-SMA, collagens I and IV, were detected using western blot analysis and IHC. The results demonstrated that in Con A-treated mice, the mRNA expression levels of ACTA2, COL1A1 and COL4A1 were increased in the liver, whereas mice treated with Ad-ACVR2A shRNA exhibited decreased expression(Fig. 3A). Similar alterations were detected in α-SMA, collagen I and IV protein expression (Fig. 3B and C). Furthermore, the enhanced phosphorylation of Smad2 in fibrotic liver tissues was suppressed when activin/ACVR2A signaling was blocked (Fig. 3D). Collectively, these data demonstrated that activation of HSCs was decreased in mice treated with Ad-ACVR2A shRNA.

Ad-ACVR2A shRNA suppresses IL-17-induced activation of primary mHSCs in vitro. In order to determine the role of the activin/ACVR2A/Smad2 pathway in immune-associated
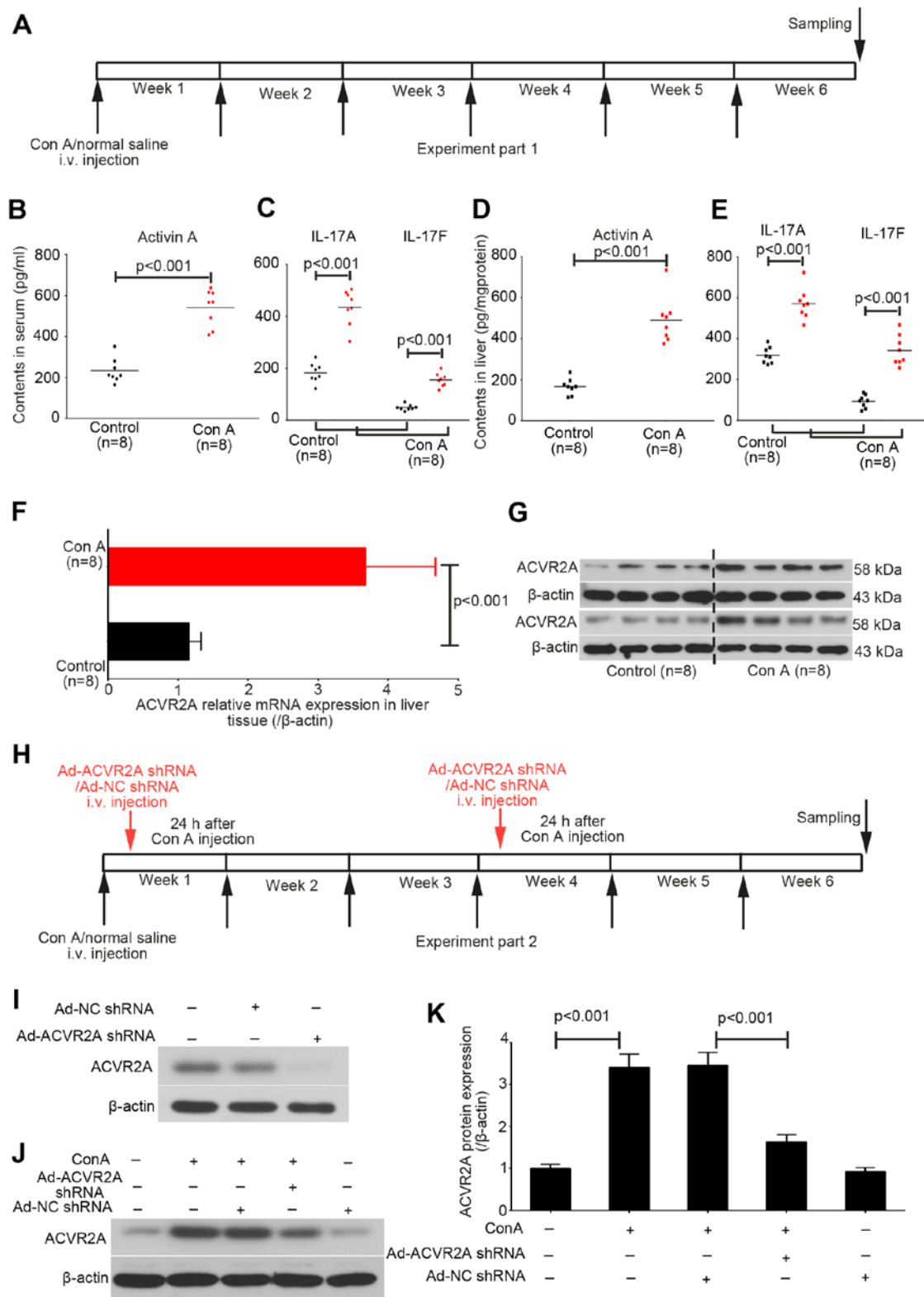
Figure 1. Chronic treatment with Con A induces activation of activin and IL-17 signaling in mouse liver. (A) Experiment part 1: Mice were administered Con A (8 mg/kg/week) for up to 6 weeks, in order to generate a model of immune-associated liver fibrosis. (B-E) Serum and liver levels of activin A, IL-17A and IL-17F were detected in mice in the control and Con A groups using specific ELISA kits. (F) mRNA and (G) protein expression levels of ACVR2A were determined using reverse transcription-quantitative polymerase chain reaction and western blot analysis, respectively. Data are expressed as the means ± standard deviation. (H) Experiment part 2: Mice in the Con A groups were administered two injections of Ad-ACVR2A shRNA or Ad-NC shRNA at the indicated timepoints. (I-K) Protein expression levels of ACVR2A were analyzed in mouse liver tissues collected from the various groups. Data are expressed as the means ± standard error. ACVR2A, activin A receptor type 2A; Con A, concanavalin A; IL-17, interleukin-17; NC, negative control; shRNA, short hairpin RNA.

liver fibrosis, primary mHSCs were isolated from normal liver samples and were treated with IL-17A and IL-17F (Fig. 4).

Following stimulation with IL-17A or IL-17F, mHSCs produced more activin A, as evidenced by ELISA (Fig. 4A, C, E and G).
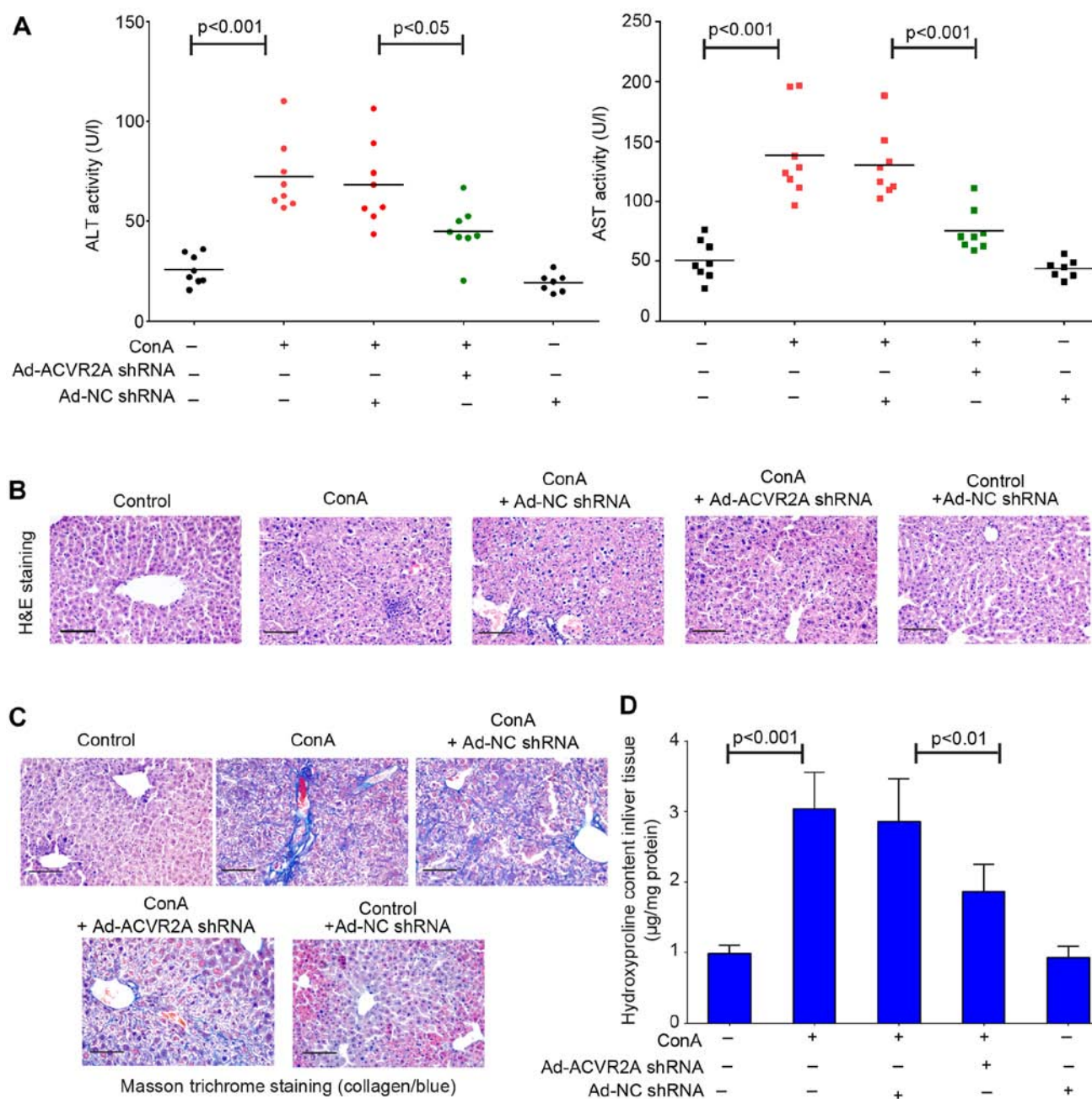
Figure 2. Knockdown of ACVR2A improves liver function and attenuates fibrosis in Con A-treated mice. (A) Activity of liver function indices ALT and AST in serum samples were determined using commercial detection kits (n=7-8/group). (B) H&E staining was applied to detect the morphological structure of the liver. (C) Hepatic fibrosis was determined using the Masson trichrome assay (fibrotic area, blue). (D) Hydroxyproline content was assessed using a commercial kit. Data are expressed as the means ± standard deviation (n=8/group). Scale bars, 100 μm. ACVR2A, activin A receptor type 2A; ALT, alanine aminotransferase; AST, aspartate aminotransferase; Con A, concanavalin A; H&E, hematoxylin and eosin; NC, negative control; shRNA, short hairpin RNA.

In addition, an increase in α-SMA was detected in mHSCs in response to IL-17 treatment (Fig. 4B, D, F and H). Furthermore, in order to disrupt activin/ACVR2A signaling in primary mHSCs, cells were infected with Ad-ACVR2A shRNA or Ad-NC shRNA for 24 h, and were then stimulated with IL-17A or IL-17F for an additional 48 h. The results demonstrated that IL-17-induced overproduction of collagens was suppressed when ACVR2A was inhibited. In addition, the expression levels of α-SMA and p-Smad2 were decreased in mHSCs infected with Ad-ACVR2A shRNA (Fig. 5). Taken together, these results suggested that knockdown of ACVR2A may inhibit IL-17-induced mHSC activation *in vitro*.

Discussion

The natural inhibitor of activin, follistatin, has been reported to attenuate CCl$_4$-induced liver fibrosis by reducing HSC proliferation and activation (27), thus suggesting that activated activin signaling may contribute to liver fibrosis. An immune imbalance is involved in liver fibrosis (1); however, the mechanisms underlying activin signaling in immune-induced liver fibrosis remain unclear. In the present study, adenovirus-mediated knockdown of ACVR2A was performed in mice treated with Con A and in primary mHSCs stimulated with IL-17. The results indicated that the suppression of activin signaling
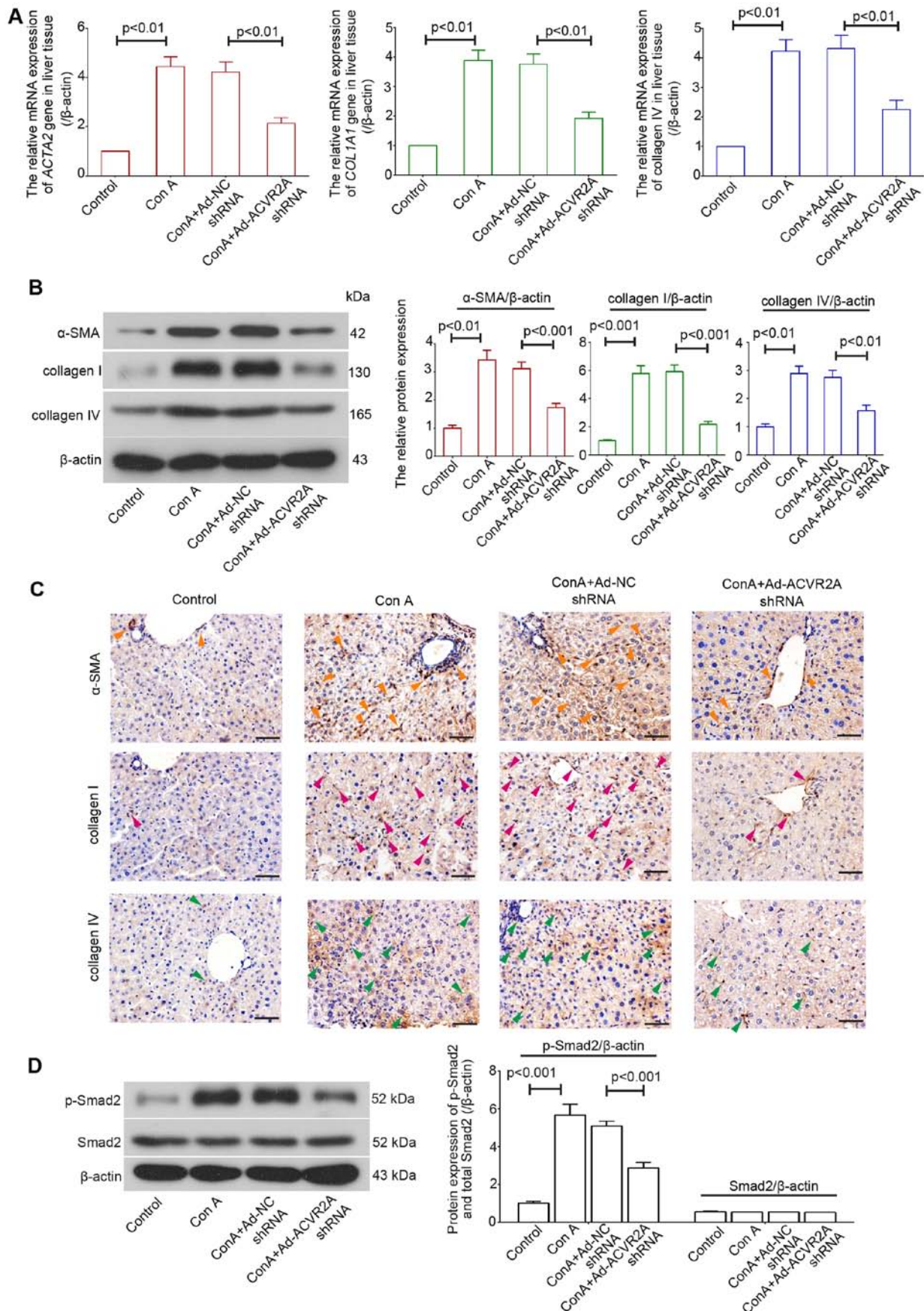
Figure 3. Knockdown of ACVR2A suppresses Con A-induced activation of hepatic stellate cells *in vivo*. (A) Relative mRNA and (B) protein expression levels of ACTA2, COL1A1 and COL4A1 were determined using reverse transcription-quantitative polymerase chain reaction and western blot analysis, respectively. (C) Immunohistochemistry was performed to detect the protein expression levels of α-SMA, collagen I and IV. Orange arrowheads, representative α-SMA-positive cells; pink arrowheads, representative collagen I-positive cells; green arrowheads, representative collagen IV-positive cells. Scale bars, 50 μm. (D) Protein expression levels of p-Smad2 and total Smad2 in liver tissues were detected using western blot analysis. Data are expressed as the means ± standard error (n=5/group). α-SMA, α-smooth muscle actin; ACVR2A, activin A receptor type 2A; Con A, concanavalin A; ; NC, negative control; p-, phosphorylated; shRNA, short hairpin RNA.
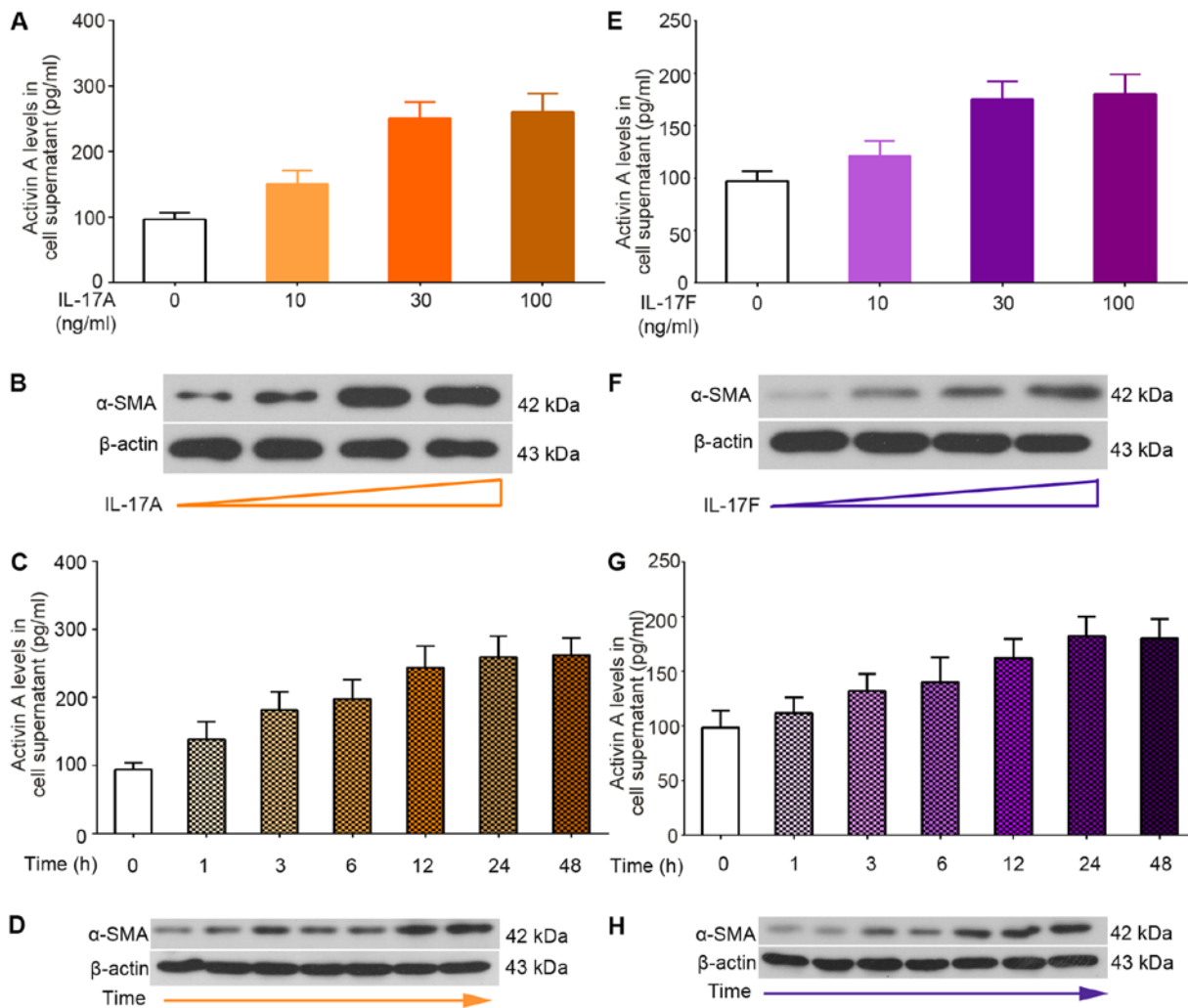
Figure 4. IL-17 induces activation of primary mHSCs *in vitro*. Recombinant mouse (A and B) IL-17A and (E and F) IL-17F (10, 30 or 100 ng/ml) were used to stimulate primary mHSCs for 48 h. In addition, mHSCs were treated with 30 ng/ml (C and D) IL-17A and (G and H) IL-17F for the indicated time periods. Activin A content in cell supernatants was determined by ELISA, and the expression levels of the marker for the activated HSCs, α-SMA, was determined by western blot analysis. Data are expressed as the means ± standard deviation (n=3/group). α-SMA, α-smooth muscle actin; IL-17, interleukin-17; mHSCs, mouse hepatic stellate cells

attenuated chronic Con A administration-induced hepatic fibrosis, in addition to preserving liver function. Collagen production in IL-17-stimulated mHSCs was also inhibited in response to ACVR2A knockdown.

Patella *et al* reported that serum levels of activin A were much higher in human subjects with chronic viral hepatitis (28), thus revealing a link between increased activin A and liver disorders. Similar to TGF-β, activins initiate signaling by binding to heterodimers, which consist of the two type II receptors: ACVR2A and activin A receptor type 2B (10). Our previous study reported that the mRNA expression levels of activin β and ACVR2A may be increased in the liver of mice following a single injection of CCl_4, and that blockade of activin signaling using a specific blocking antibody may preserve liver function (29). This previous study revealed an involvement of activin signaling in repair/regeneration-related acute liver injury. The present study aimed to further explore the role of this signaling pathway in immune-associated fibrotic liver injury.

The present study detected increased levels of activin A in the serum, and of its receptor ACVR2A in liver tissues of mice

with T-cell-mediated fibrosis. Suppression of activin signaling was achieved using adenoviruses containing ACVR2A shRNA. The results indicated that systematic delivery of Ad-ACVR2A shRNA effectively inhibited ACVR2A expression in fibrotic liver tissues. Furthermore, liver function was partly restored in response to Ad-ACVR2A shRNA, and the activation of HSCs and collagen deposition were also inhibited. George *et al* demonstrated that the TGF-β receptor antagonist is able to partly block fibrogenesis induced by ligation of the common bile duct in rats (30). These findings indicated that TGF-β may be a determinant for liver fibrosis; however, it may not be the only one. The present study suggested a pathogenic role for activated activin signaling in experimental liver fibrosis, particularly in immune-induced liver fibrosis.

Fibrotic autoimmune diseases, including primary biliary cirrhosis and systemic sclerosis, are associated with an inflammatory process in which Th17 lymphocytes serve a critical role (31). IL-17 is a proinflammatory and fibrogenic cytokine that is mainly produced by Th17 cells. In a previous study, IL-17 elevation was detected in animals with Con A-induced acute liver injury (32); similarly, in the present study, IL-17A
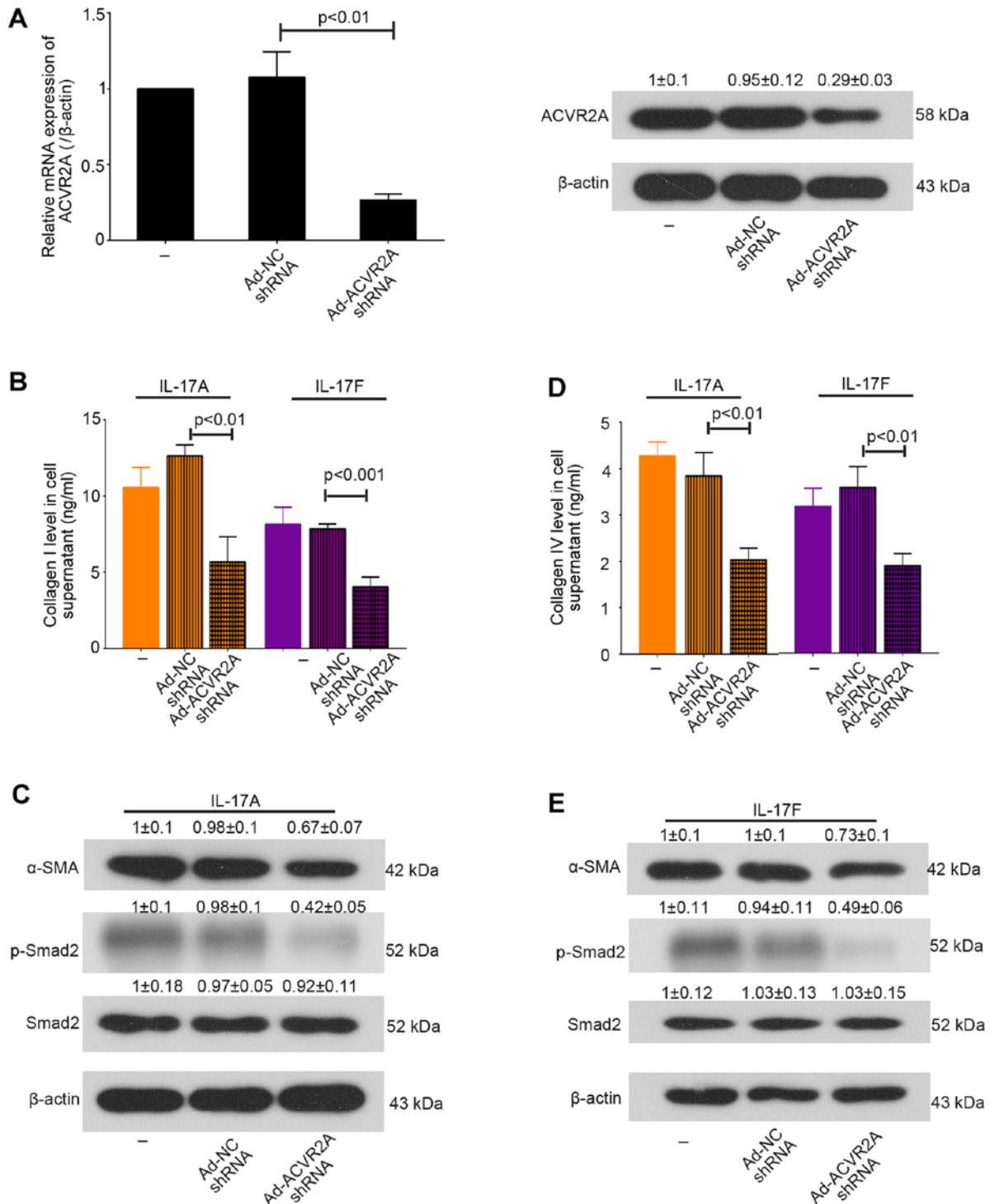
Figure 5. Ad-ACVR2A shRNA suppresses IL-17-induced activation of primary mHSCs *in vitro*. The primary mHSCs were infected with Ad-ACVR2A shRNA or Ad-NC shRNA for 24 h, and were then stimulated with recombinant IL-17A or IL-17F for an additional 48 h. (A) Knockdown efficiency of Ad-ACVR2A shRNA was confirmed in normal mHSCs by western blot analysis. (B and D) Production of collagens I and VI in cell supernatants were determined by ELISA kits. (C and E) Protein expression levels of α-SMA, p-Smad2 and total Smad2 were determined by western blot analysis. Data are expressed as the means ± standard deviation (n=3/group). α-SMA, α-smooth muscle actin; ACVR2A, activin A receptor type 2A; IL-17, interleukin-17; mHSCs, mouse hepatic stellate cells; NC, negative control; p, phosphorylated; shRNA, short hairpin RNA.

and IL-17F levels were upregulated in mice chronically treated with Con A. HSCs are considered potential target cells for IL-17, because they also express IL-17 receptors (33,34). Previous studies have indicated that IL-17s strongly stimulate the activation of HSCs; however, these studies have focused on TGF-β signaling (17,21). The production of activin A is reported to be mediated by numerous immune-related cytokines, including interferon-γ (IFN-γ) and IL-10 (35,36). Notably, in a Con A-induced liver fibrosis model, the expression levels of IFN-γ and IL-10 were increased in serum and liver samples (15). In order to exclusively study whether IL-17s affect activin signaling transduction in HSCs, and whether the interaction

between IL-17 and activin signaling impacts HSC activation, recombinant IL-17A and IL-17F were used to stimulate primary mHSCs with normal or reduced ACVR2A expression *in vitro*.

The present results were in agreement with a previous study (21), thus indicating that IL-17 may induce activation of mHSCs. TGF-β and activin A are autocrine factors, which stimulate each other's expression, thus triggering amplified fibrotic signaling in HSCs (37). Notably, in addition to TGF-β, the present study demonstrated that mHSCs generated more activin A in response to IL-17 stimulation. Furthermore, mHSCs with reduced ACVR2A expression produced less collagens in the presence of IL-17A or IL-17F; α-SMA expression was also decreased. Wada *et al* previously reported that exogenous activin A activates HSCs and increases their collagen production and α-SMA expression (37). The present findings supported the hypothesis that activated activin signaling is involved in IL-17-induced HSC activation.

Smad proteins are known as intracellular mediators for signaling transduction of TGF-β family members (38). The receptor-regulated Smads, such as Smad2, can be recruited and phosphorylated by heteromeric complexes, including activins and their receptors, and further form heterotrimers with Smad4 to relocate into the nucleus, thus regulating transcription via various promoters (10). Reportedly, exogenous activin A induces phosphorylation on Smad2 at Ser465 and Ser467 in hepatic progenitor cells (39). Phosphorylation of Smad2 in the C terminus is considered a marker of fibrogenic signaling (40). Ser465 and Ser467 are located in the C terminus of Smad2, and the phosphorylation of these sites may provide a recognition site for interaction with Smad4 (41). Therefore, due to the critical role of p-Ser465/Ser467 in Smad2 signaling activation, the present study detected p-Smad2 (Ser465/Ser467) expression. The results demonstrated that phosphorylation of these two sites induced by Con A in liver and by IL-17 in mHSCs were attenuated when activin signaling was blocked.

Notably, besides Th17 cells, other polarized CD4^{+} T-cells, including Th1, Th2 and regulatory T-cells, are critical regulators of the immune response during fibrosis (42). Further study is required to explore whether the activin A/ACVR2A/Smad2 signaling pathway is mediated by other CD4^{+} T-cells in hepatic fibrosis. Furthermore, in the presence of proinflammatory factors, including IL-1β and tumor necrosis factor-α, exogenous TGF-β1 treatment is able to promote the conversion of naive CD4^{+} T-cells into Th17 cells (43). Activin A has a synergic role with TGF-β1 (44). Notably, Ihn *et al* demonstrated that transcription of the ACVR2A gene is induced during Th17 differentiation, but not in Th1 or Th2 cells, thus suggesting that the activin/ACVR2A signaling pathway may serve a role in Th17 polarization (45). The present study focused on Th17 cell-mediated activation of HSCs; however, to fully reveal the role of activin A/ACVR2A signaling in immune-associated liver fibrosis, it will be interesting to investigate whether activated HSCs in turn mediate the polarization of CD4^{+} T-cells through this signaling pathway.

In conclusion, the present study demonstrated that activated activin A/ACVR2A/Smad2 signaling may contribute to Con A-induced hepatic fibrosis and IL-17-mediated HSC activation. Further studies are required to explore the role of this signaling pathway in the interaction between immune cells and HSCs in liver fibrosis.

Availability of data and materials

All relevant data are within the paper.

Authors' contributions

HZ conceived and wrote the study. HZ and BJ performed the experiments. HZ, BJ and YN acquired the data. HZ, BS, YX and PG performed the data analysis. All authors read and approved the final manuscript.

Ethics approval and consent to participate

The present study was approved by the Institutional Animal Care and Use committee of Mudanjiang Medical University (Mudanjiang, China).

Consent for publication

Not applicable.

Competing interests

The authors declare that they have no competing interests.

References

1. Pellicoro A, Ramachandran P, Iredale JP and Fallowfield JA: Liver fibrosis and repair: Immune regulation of wound healing in a solid organ. Nat Rev Immunol 14: 181-194, 2014.
2. Nanthakumar CB, Hatley RJ, Lemma S, Gauldie J, Marshall RP and Macdonald SJ: Dissecting fibrosis: Therapeutic insights from the small-molecule toolbox. Nat Rev Drug Discov 14: 693-720, 2015.
3. Lee YA, Wallace MC and Friedman SL: Pathobiology of liver fibrosis: A translational success story. Gut 64: 830-841, 2015.
4. Mederacke I, Hsu CC, Troeger JS, Huebener P, Mu X, Dapito DH, Pradere JP and Schwabe RF: Fate tracing reveals hepatic stellate cells as dominant contributors to liver fibrosis independent of its aetiology. Nat Commun 4: 2823, 2013.
5. Chen RJ, Wu HH and Wang YJ: Strategies to prevent and reverse liver fibrosis in humans and laboratory animals. Arch Toxicol 89: 1727-1750, 2015.
6. Seki E and Schwabe RF: Hepatic inflammation and fibrosis: Functional links and key pathways. Hepatology 61: 1066-1079, 2015.
7. Bissell DM, Roulot D and George J: Transforming growth factor beta and the liver. Hepatology 34: 859-867, 2001.
8. Nakamura T, Sakata R, Ueno T, Sata M and Ueno H: Inhibition of transforming growth factor beta prevents progression of liver fibrosis and enhances hepatocyte regeneration in dimethylnitrosamine-treated rats. Hepatology 32: 247-255, 2000.
9. Qi Z, Atsuchi N, Ooshima A, Takeshita A and Ueno H: Blockade of type beta transforming growth factor signaling prevents liver fibrosis and dysfunction in the rat. Proc Natl Acad Sci USA 96: 2345-2349, 1999.
10. Weiss A and Attisano L: The TGFbeta superfamily signaling pathway. Wiley Interdiscip Rev Dev Biol 2: 47-63, 2013.

11. Kreidl E, Oztürk D, Metzner T, Berger W and Grusch M: Activins and follistatins: Emerging roles in liver physiology and cancer. World J Hepatol 1: 17-27, 2009.

12. Sugiyama M, Ichida T, Sato T, Ishikawa T, Matsuda Y and Asakura H: Expression of activin A is increased in cirrhotic and fibrotic rat livers. Gastroenterology 114: 550-558, 1998.

13. Gold EJ, Francis RJ, Zimmermann A, Mellor SL, Cranfield M, Risbridger GP, Groome NP, Wheatley AM and Fleming JS: Changes in activin and activin receptor subunit expression in rat liver during the development of CCl₄-induced cirrhosis. Mol Cell Endocrinol 201: 143-153, 2003.

14. Fujita T, Soontrapa K, Ito Y, Iwaisako K, Moniaga CS, Asagiri M, Majima M and Narumiya S: Hepatic stellate cells relay inflammation signaling from sinusoids to parenchyma in mouse models of immune-mediated hepatitis. Hepatology 63: 1325-1339, 2016.

15. Louis H, Le Moine A, Quertinmont E, Peny MO, Geerts A, Goldman M, Le Moine O and Devière J: Repeated concanavalin A challenge in mice induces an interleukin 10-producing phenotype and liver fibrosis. Hepatology 31: 381-390, 2000.

16. Tu CT, Li J, Wang FP, Li L, Wang JY and Jiang W: Glycyrrhizin regulates CD4⁺ T cell response during liver fibrogenesis via JNK, ERK and PI3K/AKT pathway. Int Immunopharmacol 14: 410-421, 2012.

17. Meng F, Wang K, Aoyama T, Grivennikov SI, Paik Y, Scholten D, Cong M, Iwaisako K, Liu X, Zhang M, et al: Interleukin-17 signaling in inflammatory, Kupffer cells, and hepatic stellate cells exacerbates liver fibrosis in mice. Gastroenterology 143: 765-76.e1-3, 2012.

18. Song E, Lee SK, Wang J, Ince N, Ouyang N, Min J, Chen J, Shankar P and Lieberman J: RNA interference targeting Fas protects mice from fulminant hepatitis. Nat Med 9: 347-351, 2003.

19. Yu PB, Beppu H, Kawai N, Li E and Bloch KD: Bone morphogenetic protein (BMP) type II receptor deletion reveals BMP ligand-specific gain of signaling in pulmonary artery smooth muscle cells. J Biol Chem 280: 24443-24450, 2005.

20. Xu WH, Hu HG, Tian Y, Wang SZ, Li J, Li JZ, Deng X, Qian H, Qiu L, Hu ZL, et al: Bioactive compound reveals a novel function for ribosomal protein S5 in hepatic stellate cell activation and hepatic fibrosis. Hepatology 60: 648-660, 2014.

21. Tan Z, Qian X, Jiang R, Liu Q, Wang Y, Chen C, Wang X, Ryffel B and Sun B: IL-17A plays a critical role in the pathogenesis of liver fibrosis through hepatic stellate cell activation. J Immunol 191: 1835-1844, 2013.

22. Li Y, Kim BG, Qian S, Letterio JJ, Fung JJ, Lu L and Lin F: Hepatic stellate cells inhibit T cells through active TGF-β1 from a cell surface-bound latent TGF-β1/GARP complex. J Immunol 195: 2648-2656, 2015.

23. Yu MC, Chen CH, Liang X, Wang L, Gandhi CR, Fung JJ, Lu L and Qian S: Inhibition of T-cell responses by hepatic stellate cells via B7-H1-mediated T-cell apoptosis in mice. Hepatology 40: 1312-1321, 2004.

24. Weiskirchen S, Tag CG, Sauer-Lehnen S, Tacke F and Weiskirchen R: Isolation and culture of primary murine hepatic stellate cells. Methods Mol Biol 1627: 165-191, 2017.

25. Livak KJ and Schmittgen TD: Analysis of relative gene expression data using real-time quantitative PCR and the 2(-Delta Delta C(T)) Method. Methods 25: 402-408, 2001.

26. Chang J, Lan T, Li C, Ji X, Zheng L, Gou H, Ou Y, Wu T, Qi C, Zhang Q, et al: Activation of Slit2-Robo1 signaling promotes liver fibrosis. J Hepatol 63: 1413-1420, 2015.

27. Patella S, Phillips DJ, Tchongue J, de Kretser DM and Sievert W: Follistatin attenuates early liver fibrosis: Effects on hepatic stellate cell activation and hepatocyte apoptosis. Am J Physiol Gastrointest Liver Physiol 290: G137-G144, 2006.

28. Patella S, Phillips DJ, de Kretser DM, Evans LW, Groome NP and Sievert W: Characterization of serum activin-A and follistatin and their relation to virological and histological determinants in chronic viral hepatitis. J Hepatol 34: 576-583, 2001.

29. Wang DH, Wang YN, Ge JY, Liu HY, Zhang HJ, Qi Y, Liu ZH and Cui XL: Role of activin A in carbon tetrachloride-induced acute liver injury. World J Gastroenterol 19: 3802-3809, 2013.

30. George J, Roulot D, Koteliansky VE and Bissell DM: In vivo inhibition of rat stellate cell activation by soluble transforming growth factor beta type II receptor: A potential new therapy for hepatic fibrosis. Proc Natl Acad Sci USA 96: 12719-12724, 1999.

31. Fenoglio D, Bernuzzi F, Battaglia F, Parodi A, Kalli F, Negrini S, De Palma R, Invernizzi P and Filaci G: Th17 and regulatory T lymphocytes in primary biliary cirrhosis and systemic sclerosis as models of autoimmune fibrotic diseases. Autoimmun Rev 12: 300-304, 2012.

32. Chen Y, Peng H, Chen Y, Wei H, Sun R and Tian Z: CD49a promotes T-cell-mediated hepatitis by driving T helper 1 cytokine and interleukin-17 production. Immunology 141: 388-400, 2014.

33. Kolls JK and Lindén A: Interleukin-17 family members and inflammation. Immunity 21: 467-476, 2004.

34. Wang Q, Zhou J, Zhang B, Tian Z, Tang J, Zheng Y, Huang Z, Tian Y, Jia Z, Tang Y, et al: Hepatitis B virus induces IL-23 production in antigen presenting cells and causes liver damage via the IL-23/IL-17 axis. PLoS Pathog 9: e1003410, 2013.

35. Seeger P, Bosisio D, Parolini S, Badolato R, Gismondi A, Santoni A and Sozzani S: Activin A as a mediator of NK-dendritic cell functional interactions. J Immunol 192: 1241-1248, 2014.

36. González-Domínguez É, Domínguez-Soto Á, Nieto C, Flores-Sevilla JL, Pacheco-Blanco M, Campos-Peña V, Meraz-Ríos MA, Vega MA, Corbí ÁL and Sánchez-Torres C: Atypical activin A and IL-10 production impairs human CD16⁺ monocyte differentiation into anti-inflammatory macrophages. J Immunol 196: 1327-1337, 2016.

37. Wada W, Kuwano H, Hasegawa Y and Kojima I: The dependence of transforming growth factor-beta-induced collagen production on autocrine factor activin A in hepatic stellate cells. Endocrinology 145: 2753-2759, 2004.

38. Macias MJ, Martin-Malpartida P and Massagué J: Structural determinants of Smad function in TGF-β signaling. Trends Biochem Sci 40: 296-308, 2015.

39. Chen L, Zhang W, Liang HF, Zhou QF, Ding ZY, Yang HQ, Liu WB, Wu YH, Man Q, Zhang BX, et al: Activin A induces growth arrest through a SMAD- dependent pathway in hepatic progenitor cells. Cell Commun Signal 12: 18, 2014.

40. Yoshida K, Murata M, Yamaguchi T, Matsuzaki K and Okazaki K: Reversible human TGF-β signal shifting between tumor suppression and fibro-carcinogenesis: Implications of Smad phospho-isoforms for hepatic epithelial-mesenchymal transitions. J Clin Med 5: 5, 2016.

41. Souchelnytskyi S, Tamaki K, Engström U, Wernstedt C, ten Dijke P and Heldin CH: Phosphorylation of Ser465 and Ser467 in the C terminus of Smad2 mediates interaction with Smad4 and is required for transforming growth factor-beta signaling. J Biol Chem 272: 28107-28115, 1997.

42. Wynn TA: Fibrotic disease and the T(H)1/T(H)2 paradigm. Nat Rev Immunol 4: 583-594, 2004.

43. Veldhoen M, Hocking RJ, Atkins CJ, Locksley RM and Stockinger B: TGFbeta in the context of an inflammatory cytokine milieu supports de novo differentiation of IL-17-producing T cells. Immunity 24: 179-189, 2006.

44. Kang JO, Lee JB and Chang J: Cholera toxin promotes Th17 cell differentiation by modulating expression of polarizing cytokines and the antigen-presenting potential of dendritic cells. PLoS One 11: e0157015, 2016.

45. Ihn HJ, Kim DH, Oh SS, Moon C, Chung JW, Song H and Kim KD: Identification of Acvr2a as a Th17 cell-specific gene induced during Th17 differentiation. Biosci Biotechnol Biochem 75: 2138-2141, 2011.